Journal of Marine Science and Technology

Volume 22 | Issue 4 Article 9

IMPACT CHARACTERISTICS OF FREE OVER-FALL IN POOL ZONE WITH UPSTREAM BED SLOPE

Shi-I Liu
Department of Civil Engineering, National Chung Hsing University, Taichung, Taiwan, R.O.C

Jen-Yan Chen
Department of Civil Engineering, National Chung Hsing University, Taichung, Taiwan, R.O.C

Yao-Ming Hong
Department of Landscape Architecture and Environmental Planning, MingDao University, Changhua County, Taiwan, R.O.C

Hung-Shin Huang
Department of Civil Engineering, National Chung Hsing University, Taichung, Taiwan, R.O.C

Rajkumar V Raikar
Department of Civil Engineering, K. L. E. S. College of Engineering and Technology, Belgaum, India.

Follow this and additional works at: https://jmstt.ntou.edu.tw/journal

 Part of the Hydraulic Engineering Commons

Recommended Citation

Liu, Shi-I; Chen, Jen-Yan; Hong, Yao-Ming; Huang, Hung-Shin; and Raikar, Rajkumar V (2014) "IMPACT CHARACTERISTICS OF FREE OVER-FALL IN POOL ZONE WITH UPSTREAM BED SLOPE," *Journal of Marine Science and Technology*: Vol. 22 : Iss. 4 , Article 9.
DOI: 10.6119/JMST-013-0604-1
Available at: https://jmstt.ntou.edu.tw/journal/vol22/iss4/9

This Research Article is brought to you for free and open access by Journal of Marine Science and Technology. It has been accepted for inclusion in Journal of Marine Science and Technology by an authorized editor of Journal of Marine Science and Technology.

IMPACT CHARACTERISTICS OF FREE OVER-FALL IN POOL ZONE WITH UPSTREAM BED SLOPE

Acknowledgements

The authors would like to thank the research support from the National Science Council of the Republic of China (project number 102-2313-B-451-001 and 99-2221-E-005-044).

This research article is available in Journal of Marine Science and Technology: https://jmstt.ntou.edu.tw/journal/vol22/iss4/9

Journal of Marine Science and Technology, Vol. 22, No. 4, pp. 476-486 (2014)
DOI: 10.6119/JMST-013-0604-1

IMPACT CHARACTERISTICS OF FREE OVER-FALL IN POOL ZONE WITH UPSTREAM BED SLOPE

Shi-I Liu[1], Jen-Yan Chen[1], Yao-Ming Hong[2], Hung-Shin Huang[1], and Rajkumar V. Raikar[3]

Key words: open channel flow, Drop structures, free over-fall, impact characteristics.

ABSTRACT

This paper presents the theoretical equations for the impact characteristics of free over-fall (ICFOF) in the pool zone with sloping upstream bed. The various impact characteristics considered are the brink depth, the impact position and impact angle, the tail water depth and the depth of water pool. In order to overcome the complexity in determining the ICFOF, they were expressed in dimensionless forms as functions of upstream bed slope (UBS), upstream Froude number and Drop number. The multiple regression analysis was used to obtain the empirical expressions for the ICFOF using the laboratory experimental results. It was found that the dimensionless brink depth decreases with an increase in upstream Froude number and UBS. With the increase in both the Drop number and UBS, the dimensionless impact position increases, while the impact angle decreases. On the other hand, the dimensional tail water depth and the dimensional depth of water pool vary directly with the Drop number and inversely with the UBS. In addition, the empirical equations proposed for horizontal upstream slope were compared with those of previous investigators. Further, a parameter called slope effect ratio is defined to state the effect of UBS on the ICFOF. Moreover, the empirical equation derived in this study can be used to design the structure of downstream apron practically. An example illustrates the calculation of the impact position/ tail water depth for downstream apron.

Paper submitted 10/02/12; revised 05/06/13; accepted 06/04/13. Author for correspondence: Yao-Ming Hong (e-mail: blueway@mdu.edu.tw).
[1] Department of Civil Engineering, National Chung Hsing University, Taichung, Taiwan, R.O.C.
[2] Department of Landscape Architecture and Environmental Planning, MingDao University, Changhua County, Taiwan, R.O.C.
[3] Department of Civil Engineering, K. L. E. S. College of Engineering and Technology, Belgaum, India.

I. INTRODUCTION

For the purpose of river regulation, slope adjustment and for water intake stabilization, hydraulic engineers usually employ hydraulic structures such as weirs or check dams in rivers. However, these structures usually produce a large elevation difference between upstream and downstream sides resulting into a free over-fall flow, which may induce scour on the downstream of the hydraulic structure and damage it eventually. Previously, many researchers studied the impact characteristics of free over-fall flow. In general, the research topics on free over-fall flow include shape of scour hole, impact position, impact force, etc. Stein and Julien [11] showed that the scour volume per unit width at any time can be expressed as twice the square of the maximum scour depth at the corresponding time for the cohesive and non-cohesive sediments. Chen and Hong [3] used two types of sands, which include uniform and graded one, to simulate the bed material downstream of the weir phenomena due to free over-fall flows. On the other hand, Chamani and Beirami [1], Tokyay and Yildiz [12], Hong *et al*. [7] and Chen *et al*. [4] investigated the impact characteristics of free over-falls (ICFOF). Chamani and Beirami [1] developed an empirical equation to estimate the relative energy loss at drops for supercritical approaching flows. Tokyay and Yildiz [12] used experimental data to analyze the characteristics of supercritical flow at a vertical drop in a rectangular channel. However, Hong *et al.* [7] presented regression and semi-theoretical models to predict the drop force and the drop length of a free-falling nappe at an aerated straight-drop spillway. On the other hand, Chen *et al*. [4] developed the theoretical equations for impact force and impact position of free over-fall flow on a sloping downstream slope.

In all the above-mentioned studies, the upstream bed slope (UBS) of the free over-fall was considered horizontal, which discharge horizontal jet. Hence, all the ICFOF flow studied were with horizontal upstream bed. However, after the construction of hydraulic structure, the entire bed load and in particular coarse sediments are not transported to the

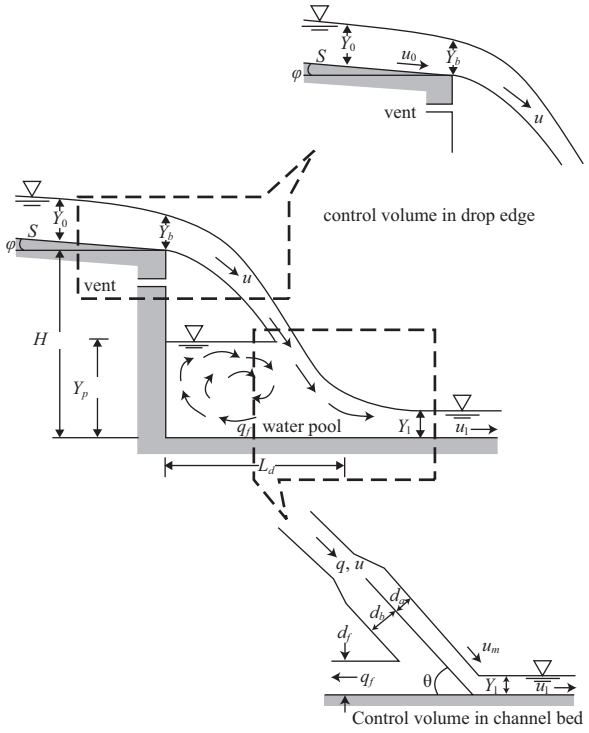

Fig. 1. Schematic diagram of free over-fall flow with UBS.

downstream side. As a consequence of the accumulation of the sediment on the upstream side of the structure, the upstream channel bed slope rises. This will change the inclination of free over-fall flow into an oblique jet, and hence modify the impact position and impact force of free over-fall flow on the downstream side. Therefore, the present study aims at the development of empirical equations for the prediction of the ICFOF in pool zone with UBS. Based on the theoretical analysis, the UBS and Drop number were selected as the independent variables of empirical equations. A series of laboratory experiments were conducted to evaluate the influencing factors of UBS for ICFOF. Further, Multiple Regression Analysis (MRA) is used to develop the empirical equations.

II. THEORETICAL ANALYSIS

1. Impact Characteristics

The schematic diagram of free over-fall with UBS and horizontal downstream bed is depicted in Fig. 1, in which H is the drop height, Y_b is the brink depth, L_d is the impact position, θ is an impact angle, Y_1 is the tail water depth and Y_p is the pool water depth. Due to steep inclination of upstream bed φ, the supercritical flow occurs in the upstream channel, and the upstream water depth Y_0 will be smaller than the critical water depth Y_c. The course of free over-fall is divided into two control volumes along the water nappe as shown in Fig. 1. Assuming the upstream energy correction coefficient α_i and the momentum correction factor β_i equal to 1, the ICFOF can be derived as follows [8, 10, 13]:

1) Brink Depth (Y_b)

Using the law of momentum conservation between approaching section and brink, one can write the following equation:

$$\frac{(Y_0\cos\varphi)^2}{2}+\frac{\beta_1 q^2}{gY_0}=\frac{Y_b^2}{2}+\frac{\beta_2 q u_b}{g} \tag{1a}$$

where q is the discharge per unit width, g is the gravitational acceleration, u_b is the velocity in the drop edge (= q/Y_b), and β_1 and β_2 are the moment correction factor at the approaching section and at brink, being equal to 1. Eq. (1a) can be rearranged to obtain brink depth as

$$Y_b=\frac{2Y_0}{F_0^{-2}\cos^2\varphi+2} \tag{1b}$$

where F_0 is the Froude Number of upstream channel (= $u_0/\sqrt{gY_0\cos\varphi}$).

2) Impact Position (L_d)

Using Newton's laws of motion, the two dimensional trace of water nappe can be expressed by

$$X=u_b\cos\varphi * t \tag{2a}$$

$$Y=\frac{Y_b}{2}-\frac{1}{2}gt^2-u_b\sin\varphi * t \tag{2b}$$

where X and Y are the horizontal and vertical coordinates of impact position of the nappe from the drop edge, respectively and t is the time taken by the water nappe to travel from the drop edge to the impact position. Substituting Eq. (2a) into Eq. (2b), yields

$$Y=\frac{Y_b}{2}-SX-\frac{g}{2\left(u_b\cos\varphi\right)^2}X^2 \tag{2c}$$

where S is the UBS (= $\tan\varphi$). Assuming rectangular channel, the critical depth of upstream channel is $Y_c=(q^2/g)^{1/3}$ and the horizontal critical velocity is $u_c=(gY_c)^{1/2}$. From Eq. (2c) the impact position L_d can be expressed as

$$L_d=\frac{q^{2/3}\left(-S+\sqrt{S^2+\overline{Y_b}^2\left(\frac{2Hg^{1/3}}{q^{2/3}}+\overline{Y_b}\right)\left(1+S^2\right)}\right)}{\overline{Y_b}^2 g^{1/3}\left(1+S^2\right)} \tag{2d}$$

where $\overline{Y_b}=Y_b/Y_c=u_c/u_b$.

3) Impact Angle (θ)

Using the law of energy conservation with UBS, the following equation can be obtained

$$H + Z_n + \frac{\alpha_1 u_0^2}{2g} + Y_0 \cos\varphi = y + \frac{\alpha_3 u^2}{2g} \tag{3a}$$

where Z_n is the bed elevation above drop edge. Because the distance between measured position of upstream water depth and the drop edge equal to 0.3 m, $Z_n = 0.3S$, y is the nappe depth impacting on downstream side of drop ($\cong 0$) and α_1 and α_3 are the energy correction coefficient at the approaching section and downstream of the brink, being equal to 1. Rearranging Eq. (3a), the impacting velocity u of water nappe on the downstream of the drop is written as

$$u = \left[2g\left(H + 0.3S + \frac{q^2}{2gY_0^2} + Y_0 \cos\varphi \right) \right]^{1/2} \tag{3b}$$

Using the law of horizontal momentum conservation ($\Sigma F_x = 0$)

$$\frac{1}{2}\rho g\left(Y_0 \cos\varphi\right)^2 = \rho q\left(u\cos\theta - u_0 \cos\varphi\right) \tag{3c}$$

where ρ is the water density. Substituting Eq. (3b) into Eq. (3c), the impact angle θ can be expressed as

$$\theta = \cos^{-1}\left[\frac{0.5g\left(Y_0\cos\varphi\right)^2 + \frac{q^2}{Y_0}\cos\varphi}{q\sqrt{2g\left(H + 0.3S + \frac{q^2}{2gY_0^2} + Y_0\cos\varphi \right)}} \right] \tag{3d}$$

4) Tail Water Depth (Y_1)

According to the experimental observation (Fig. 1), the following flow conditions were assumed:

(a) When water nappe impacts the downstream channel bed, a discharge per unit width q_f from water pool will be mixed up into the water nappe to increase the nappe discharge into ($q + q_f$) with corresponding constant velocity u_m.
(b) When steady flow occurs, the discharge flowing into water pool is q_f, and the discharge flowing into downstream is q. Therefore, under the ideal flow condition, there is always a repeated rotary discharge q_f occurring in the water pool. Further, The nappe in the water pool is considered to be divided into two parts: (i) the width of outside part d_a with a discharge per unit of q; and (ii) the width of inside part d_b with a repeated rotary discharge per unit width q_f. The tail water depth $Y_1 = d_a$ and $d_f = d_b$. From the law of momentum conservation at the downstream bed, it yields

$$\rho u_m^2\left(d_a + d_b\right)\cos\theta = \rho u_m^2 d_a - \rho u_m^2 d_f \tag{4a}$$

where u_m is the average velocity in the mixing section of nappe and repeated rotary flow of water pool. Substituting $d_f = d_b$, and rearranging,

$$\frac{d_b}{d_a} = \frac{1-\cos\theta}{1+\cos\theta} \tag{4b}$$

By continuity equation,

$$\frac{q_f}{q} = \frac{q_b}{q} = \frac{u_m \times d_b}{u_m \times d_a} \tag{4c}$$

Substituting Eq. (4b) it results

$$q_f = \frac{1-\cos\theta}{1+\cos\theta} q \tag{4d}$$

Hence, q_f will be the function of q.

Using momentum equation prior to impact and after impact, the following equation can be obtained

$$\rho q \beta_3 u = \rho\left(q + q_f\right)\beta_4 u_m = \rho\left(q + \frac{1-\cos\theta}{1+\cos\theta} q\right)\beta_4 u_m \tag{4e}$$

where β_3 and β_4 are the moment correction factor before and after the impact of jet, considered as 1. Therefore,

$$u_m = \frac{u}{2}\left(1+\cos\theta\right) \tag{4f}$$

From continuity equation, the velocity in downstream $u_1 = u_m$. By momentum conservation, one can write

$$\frac{Y_1}{Y_c} = \frac{u_c}{u_1} \tag{4g}$$

Finally, the tailwater depth Y_1 can be obtained by rearranging Eq. (4g) with substitution of $u_1 = u_m$ as

$$Y_1 = \frac{2q}{\sqrt{2g\left(H + 0.3S + \frac{q^2}{2gY_0^2} + Y_0\cos\varphi \right)} + \frac{\frac{g\left(Y_0\cos\varphi\right)^2}{2} + \frac{q^2}{Y_0}\cos\varphi}{q}} \tag{4h}$$

5) Depth of Water Pool (Y_p)

Assuming steady flow and static pressure distribution at the drop edge (Fig. 1), the momentum conservation in horizontal direction ($\Sigma F_x = 0$) between upstream section and downstream

of the brink can be written as

$$\rho q\beta_3 u\cos\theta = \rho q\beta_1 u_0\cos\varphi + \frac{1}{2}\rho g\left(Y_0\cos\varphi\right)^2 \qquad (5a)$$

The momentum equation in the control volume of channel bed (Fig. 1) can be expressed as

$$\rho q\beta_3 u\cos\theta + \frac{1}{2}\rho g Y_p^2 = \rho q\beta_5 u_1 + \frac{1}{2}\rho g Y_1^2 \qquad (5b)$$

where β_5 is the moment correction factor (= 1) in the downstream channel bed. Rearranging Eq. (5b) and using Eq. (4h), the depth of water pool is

$$Y_p = \sqrt{Y_1^2 - \left(Y_0\cos\varphi\right)^2 + \frac{2q^2}{g}\left(\frac{1}{Y_1} - \frac{\cos\varphi}{Y_0}\right)} \qquad (5c)$$

In generally, if the upstream Froude number, Drop number D (= q^2/gH^3) and UBS are known, the ICFOF can be calculated to provide the reference of structure design for free over-fall flow.

2. Development of Dimensionless ICFOF and Empirical Formulas

Although the ICFOF can be calculated by theoretical equations, the complexities of theoretical equations will induce the difficulties in application. Therefore, simple equations such as empirical equations obtained by multiple regression analysis (MRA) should be more convenient in application than theoretical equations. This study reduced the general form of empirical equations as follows:

1) Dimensionless Brink Depth ($\overline{Y_b}$)

From Eq. 1(b), dividing Y_b by Y_{cu}, the dimensionless brink depth $\overline{Y_b}$ can be written as

$$\overline{Y_b} = \frac{Y_b}{Y_c} = \frac{2Y_0}{Y_c(F_0^{-2}\cos^2\varphi + 2)} \qquad (6)$$

As Y_c is constant for particular discharge q and Y_0 is dependent on the value of upstream Froude number F_0, the dimensionless brink depth $\overline{Y_b}$ can be expressed as the function of UBS S and F_0:

$$\overline{Y_b} = f_1\left(S, F_0\right) \qquad (7a)$$

Assuming the existence of either power or exponential relationship between $\overline{Y_b}$, F_0 and S, $\overline{Y_b}$ can be written as:

$$\overline{Y_b} = a_1 \cdot F_0^{b_1} \cdot e^{c_1 S} \qquad (7b)$$

where a_1, b_1 and c_1 are constant.

2) Dimensionless Impact Position ($\overline{L_d}$)

Dividing L_d from Eq. 2(d) by H, the dimensionless impact position $\overline{L_d}$ is obtained as

$$\overline{L_d} = \frac{L_d}{H} = \frac{D^{1/3}\left(-S + \sqrt{S^2 + \overline{Y_b}^2\left(2D^{-1/3} + \overline{Y_b}\right)\left(1+S^2\right)}\right)}{\overline{Y_b}^2\left(1+S^2\right)} \qquad (8)$$

where D is Drop number (= q^2/gH^3). On the other hand, using Buckingham π-theorem, Hong *et al.* [7] derived that $\overline{L_d}$ is a function of upstream channel bed slope S and Drop number D as

$$\overline{L_d} = f_2\left(S, D\right) \qquad (9a)$$

and an empirical formula can be expressed as

$$\overline{L_d} = a_2 \cdot D^{b_2} \cdot e^{c_2 S} \qquad (9b)$$

where a_2, b_2 and c_2 are constant.

3) Impact Angle (θ)

Substituting critical depth Y_c in Eq. 3(d) by normal depth Y_0, the impact angle θ can be expressed as

$$\theta = \cos^{-1}\left[\frac{0.5g\left(Y_0\cos\varphi\right)^2 + \frac{q^2}{Y_0}\cos\varphi}{q\sqrt{2gH\left(1 + \frac{0.3S}{H} + \frac{DH^2}{2Y_0^2} + \frac{Y_0\cos\varphi}{H}\right)}}\right] \qquad (10)$$

It is also assumed the impact angle θ is a function of upstream channel bed slope S and Drop number D. Hence,

$$\theta = f_3\left(S, D\right) \qquad (11a)$$

and the corresponding empirical formula is

$$\theta = a_3 \cdot D^{b_3} \cdot e^{c_3 S} \qquad (11b)$$

where a_3, b_3 and c_3 are constant.

4) Dimensionless Tail Water Depth ($\overline{Y_1}$)

From Eq. 4(h), the dimensionless tail water depth $\overline{Y_1}$ (= Y_1/H) is

$$\overline{Y_1} = \frac{Y_1}{H} = \frac{2}{\sqrt{\frac{2}{D}\left(1+\frac{0.3S}{H}+\frac{DH^2}{2Y_0^2}+\frac{Y_0\cos\varphi}{H}\right)+\frac{(Y_0\cos\varphi)^2}{2DH^2}+\frac{H\cos\varphi}{Y_0}}} \tag{12}$$

Assuming the $\overline{Y_1}$ is a function of upstream channel bed slope S and Drop number D the relationship can be written as

$$\overline{Y_1} = f_4(S, D) \tag{13a}$$

which can be expressed as:

$$\overline{Y_1} = a_4 \cdot D^{b_4} \cdot e^{c_4 S} \tag{13b}$$

where a_4, b_4 and c_4 are constant.

5) Dimensionless Depth of Water Pool ($\overline{Y_p}$)

The dimensionless depth of water pool $\overline{Y_p} = (Y_p / H)$ can be written from Eq. 5(c) as:

$$\overline{Y_p} = \frac{Y_p}{H} = \sqrt{\left(\frac{Y_1}{H}\right)^2 - \left(\frac{Y_0\cos\varphi}{H}\right)^2 + 2DH\left(\frac{1}{Y_1}-\frac{\cos\varphi}{Y_0}\right)} \tag{14}$$

Expressing $\overline{Y_p}$ as a function of upstream channel bed slope S and Drop number D

$$\overline{Y_p} = f_5(S, D) \tag{15a}$$

or

$$\overline{Y_p} = a_5 \cdot D^{b_5} \cdot e^{c_5 S} \tag{15b}$$

where a_5, b_5 and c_5 are constant.

All the coefficients a_i, b_i and c_i (i = 1 to 5) can be determined by experimental data. In general, if the three physical parameters such as UBS S, upstream Froude number F_0 and Drop number D are known, all of the ICFOF can be calculated. In addition, for horizontal upstream slope, ICFOF are only the functions of Drop number D.

3. Slope Effect Ratio

The slope effect ratio (SER) δ may be defined as

$$\delta = A_{(S>0)} / A_{(S=0)} \tag{16}$$

where $A_{(S>0)}$ is a impact characteristics with UBS $S > 0$ and $A_{(S=0)}$ is the same impact characteristics with UBS $S = 0$. The SER can be used to illustrate the change ratio of impact characteristics due to UBS. Various SER for dimensionless ICFOF are defined as follows.

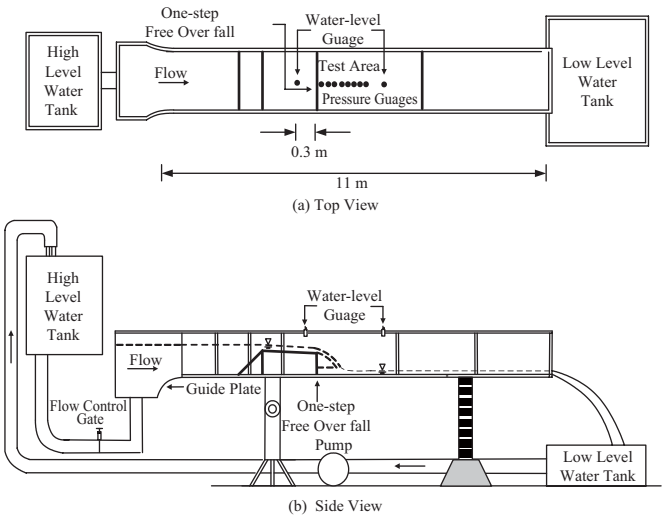

Fig. 2. Schematic diagram of free over-fall flow with UBS.

$$\delta_{\overline{Y_b}} = e^{c_1 S} \tag{17a}$$

$$\delta_{\overline{L_d}} = e^{c_2 S} \tag{17b}$$

$$\delta_{\theta} = e^{c_3 S} \tag{17c}$$

$$\delta_{\overline{Y_1}} = e^{c_4 S} \tag{17d}$$

$$\delta_{\overline{Y_p}} = e^{c_5 S} \tag{17e}$$

Eqs. (17a)-(17e) show that SER is the function of exponential power of UBS S. A larger value of UBS S induces a larger SER.

III. EXPERIMENTATION

Experiments were carried out in a glass-sided laboratory channel 11 m long, 0.3 m wide and 0.4 m deep, at the National Chung Hsing University, Taiwan. The bottom slope of the channel was adjustable. The flow rate in the channel was accurately controlled by a constant head tank with a variable-speed electronic controller. Water is recirculated from a low level water tank to a high level constant head water tank by a pump. An ultrasonic water-level gauge, RPS-401A, was used to measure the water depth. Fig. 2 illustrates the experimental setup. The vertical drop models were made of high density acrylic fibre plates. Four drop models of height H = 0.3 m, 0.25 m, 0.2 m and 0.15 m were used in the present study. The air cavity between the drop wall and bottom of the nappe was well ventilated by means of holes made in the drop wall (see Fig. 2). The pressure measuring system consists of 8 pressure gauges mounted in the middle of a high density acrylic fibre

Table 1. Range of experimental conditions.

Test Conditions	Conditions
Upstream channel bed slope, S (%)	0 (Control group), 2, 4, 6
Drop height, H (m)	0.3, 0.25, 0.2, 0.15
Unit width flow rate, q (m^3/s/m)	0.0079-0.0428
Upstream Froude number, F_0	1.432-4.887
Drop number, D ($\times 10^{-4}$)	2.36-552.30

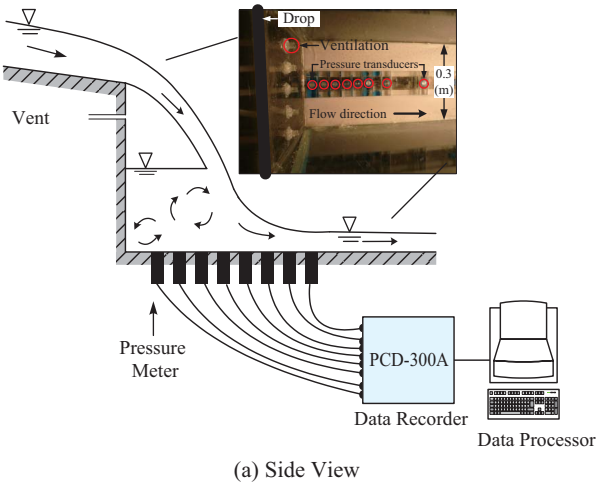

Fig. 3. Layout of pressure measuring system.

plate. The pressure gauges were located along the centerline of the channel and their top levels were kept on the channel bed surface in order to sense the impact pressure of free over-fall. Fig. 3 illustrates the layout of pressure measuring system. When free-falling nappe impacted the downstream bed surface, the impact pressure sensed by the pressure gauges (KYOWA BP-500GRS) was sent to the data recorder, which could save and record the real-time impact pressure. The maximum value of impact pressures obtained by the pressure gauges is the impact position (L_d). i.e. L_d is the distance between the drop wall and the position of the maximum value of the impact pressure.

The experiments were conducted under steady flow condition. The measurement position of impact pressure was located along the center line of the channel in order to eliminate the effect of friction due to glass walls. Total 64 experiments were performed to obtain ICFOF. Table 1 furnishes the range of the experimental data. The UBS S ranges between 0-6%, the drop height H ranges from 0.15 m-0.30 m, the unit discharge q is in the range of 0.0079 m^3/s/m-0.0428 m^3/s/m. The

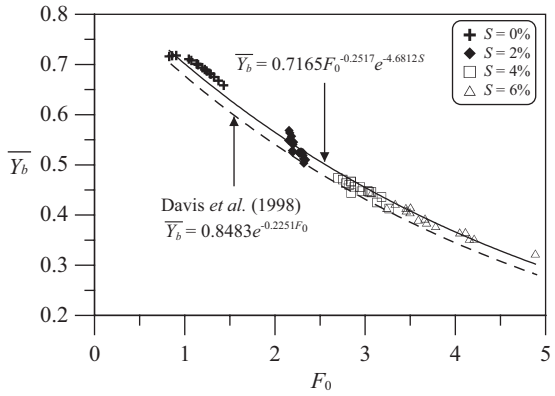

Fig. 4. Variation of dimensionless brink depth with upstream Froude number for various UBS.

corresponding ranges of upstream Froude number F_0 and the Drop number D were 1.432-4.887 and $2.36 \times 10^{-4} - 552.30 \times 10^{-4}$, respectively. The values of Froude number indicated that the upstream flow condition was supercritical flow, which supported the assumption made in the theoretical analysis.

IV. ESTABLISHMENT OF EMPIRICAL FORMULAE AND DISCUSSIONS

The laboratory experimental results were used to adopt the multiple regression analysis (MRA) to obtain the coefficients of empirical formulae.

1. Brink Depth

The laboratory experimental data for different UBS S = 0-6% are used to obtain the multiple regression equation for dimensionless brink depth $\overline{Y_b}$ following Eq. (7b). The equation for dimensionless brink depth with coefficient of determination value $R^2 = 0.983$ is

$$\overline{Y_b} = 0.7165F_0^{-0.252}e^{-4.681S} \tag{18}$$

Eq. (18) indicates that with an increase in Froude number F_0 as well as the UBS S, the dimensionless brink depth $\overline{Y_b}$ decreases. Fig. 4 depicts the variation of dimensionless brink depth $\overline{Y_b}$ with Froude number F_0 for various UBS S.

The equation proposed by Davis *et al*. [6] with UBS S = 0.33-3.33% is also shown in Fig. 4. From Fig. 4, it can be observed that Eq. (18) fits very well with the experimental data and compares close with equation of Davis *et al.* [6]. Hence it can be used to determine the brink depth Y_b.

2. Impact Position

The experimental results are used to obtain the multiple regression equation for the dimensionless impact position $\overline{L_d}$. Although Eq. (9b) expresses the dimensionless impact position as a function of Drop number D and UBS S, two types of

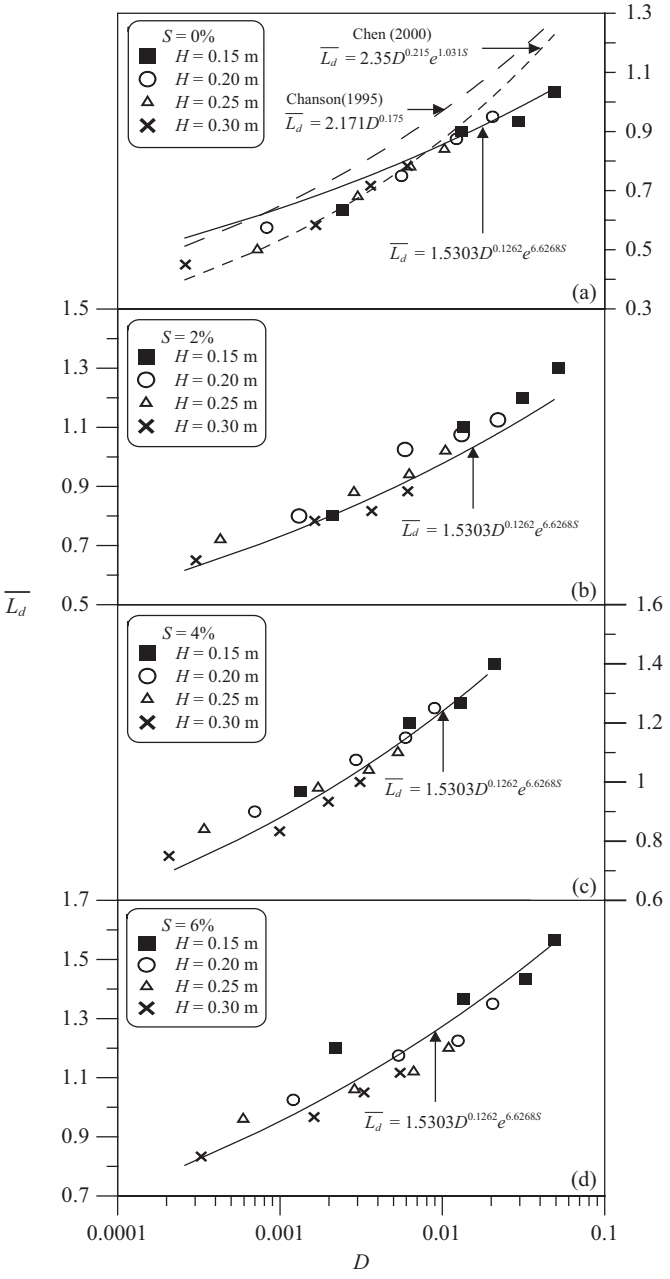

Fig. 5. Variation of dimensionless impact position with Drop number for various UBS.

equations are developed for the $\overline{L_d}$ in the present study. Initially, the multiple regression equation for the dimensionless impact position $\overline{L_d}$ are obtained by considering only the Drop number D and the equations for different UBS are:

$$\overline{L_d} = 1.5303D^{0.126} \quad \text{for } S = 0 \tag{19a}$$

$$\overline{L_d} = 1.7472D^{0.126} \quad \text{for } S = 2\% \tag{19b}$$

$$\overline{L_d} = 1.9948D^{0.126} \quad \text{for } S = 4\% \tag{19c}$$

$$\overline{L_d} = 2.2775D^{0.126} \quad \text{for } S = 6\% \tag{19d}$$

In Eqs. (19a)-(19d), exponent b_2 of Drop number D is constant and equal to 0.126 for all values of UBS, however, the constant a_2 increases with an increase in the UBS up to 4%, while it decreases for S = 6%. On the other hand, Eq. (20) represents the multiple regression equation for the dimensionless impact position $\overline{L_d}$ as s function of Drop number D and UBS S.

$$\overline{L_d} = 1.5303D^{0.126}e^{6.627S} \tag{20}$$

Eq. (20) shows that the large values of Drop number D and UBS S induce a greater dimensionless impact position $\overline{L_d}$. The correlation of $\overline{L_d}$ with D and S is considerably as expressed by the correlation coefficient R^2 = 0.941. Fig. 5 presents the variation of dimensionless impact position $\overline{L_d}$ with Drop number D for different UBS S. The experimental data collapse on the curve of $\overline{L_d}$ obtained by Eq. (20). In addition, the dimensionless impact position $\overline{L_d}$ computed by equations of Chanson [2] and Chen [5] for UBS S = 0 are shown in Fig. 5(a). From Fig. 5(a), it is clear that the $\overline{L_d}$ determined by Chanson [2] equation is larger than the experimental values, while that from Chen [5] equation is more close to the experimental results. The Chanson [2] equation over predicts the $\overline{L_d}$ as it does not incorporate the effect of UBS S. However, the Chen's [5] results are comparable with the present study.

3. Impact Angle

The multiple regression equation [following Eq. (11b)] for impact angles θ obtained by the laboratory experimental data (with R^2 = 0.913) is

$$\theta = 47.4888D^{-0.057}e^{-2.563S} \tag{21}$$

The variation of impact angles θ with Drop numbers D presented in Fig. 6 shows decrease in impact angle θ with an increase in the Drop number D. Also, for the same drop number D, the impact angle θ decreases with an increase in UBS S. The variations of θ for different UBS computed by Eq. (21) are expressed in Eq. (22a)-22(d).

$$\theta = 47.4888D^{-0.057} \quad \text{for } S = 0 \tag{22a}$$

$$\theta = 45.1559D^{-0.057} \quad \text{for } S = 2\% \tag{22b}$$

$$\theta = 42.8615D^{-0.057} \quad \text{for } S = 4\% \tag{22c}$$

$$\theta = 40.7198D^{-0.057} \quad \text{for } S = 6\% \tag{22d}$$

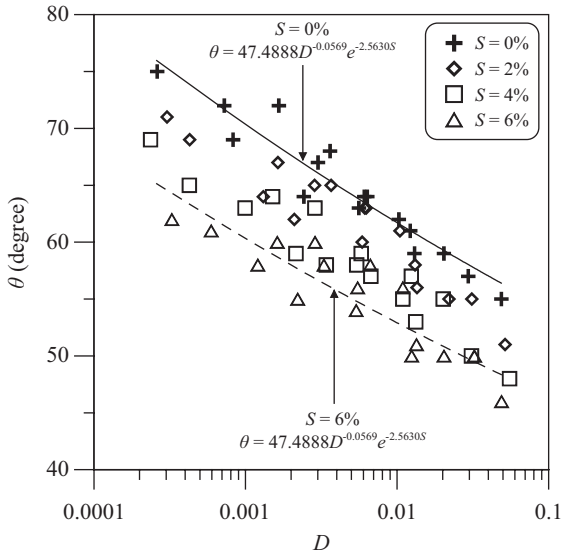

Fig. 6. Variation of impact angle with Drop number for various UBS.

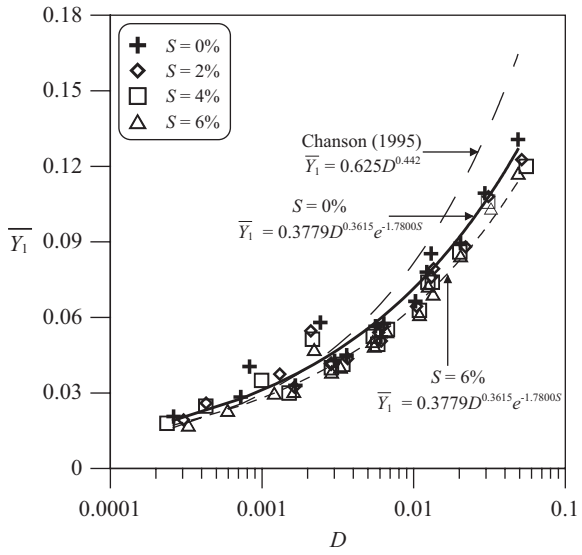

Fig. 7. Variation of dimensionless tail water depth with Drop number for various UBS.

4. Tail Water Depth

Following Eq. (13b), the multiple regression equation for dimensionless tail water depth $\overline{Y_1}$ is obtained as

$$\overline{Y_1} = 0.3779 D^{0.362} e^{-1.780 S} \tag{23}$$

Eq. (23) depicts that the dimensionless tail water depth $\overline{Y_1}$ increases with an increase in Drop number D decrease in UBS S. The variation of $\overline{Y_1}$ with Drop number D and UBS S is shown in Fig. 7. In addition, the relationship proposed by Chanson [2] between dimensionless tail water depth $\overline{Y_1}$ and Drop number D for S = 0 shown in Fig. 7, indicates the over estimation of dimensionless tail water depth $\overline{Y_1}$ for drop number $D > 0.003$. However, Eq. (23) fits the present experimental data promisingly with R^2 = 0.967. Further, the relationships between dimensionless tail water depth and Drop number for various UBS are

$$\overline{Y_1} = 0.3779 D^{0.362} \quad \text{for } S = 0 \tag{24a}$$

$$\overline{Y_1} = 0.3647 D^{0.362} \quad \text{for } S = 2\% \tag{24b}$$

$$\overline{Y_1} = 0.3519 D^{0.362} \quad \text{for } S = 4\% \tag{24c}$$

$$\overline{Y_1} = 0.3396 D^{0.362} \quad \text{for } S = 6\% \tag{24d}$$

5. Depth of Water Pool

The multiple regression equation for dimensionless depth of water pool $\overline{Y_p}$ can be expressed as

$$\overline{Y_p} = 1.0234 D^{0.241} e^{-1.157 S} \tag{25}$$

From Eq. (25) it is clear that the dimensionless depth of water pool $\overline{Y_p}$ varies directly with Drop number D and indirectly with UBS S. Fig. 8 illustrates the dependency of dimensionless depth of water pool $\overline{Y_p}$ on Drop number D for different UBS S. In addition, the equations proposed by Rand [9] and Chanson [2] are also shown in Fig. 8 (a) for S = 0, which illustrate the close correspondence of Eq. (25) with that of Rand [9] and Chanson[2].

Further, Eq. (25) predicts the dimensionless depth of water pool $\overline{Y_p}$ very well having correlation coefficient R^2 = 0.992. Now, for different UBS S, the expressions for dimensionless depth of water pool $\overline{Y_p}$ can be expressed as

$$\overline{Y_p} = 1.0234 D^{0.241} \quad \text{for } S = 0 \tag{26a}$$

$$\overline{Y_p} = 0.9999 D^{0.241} \quad \text{for } S = 2\% \tag{26b}$$

$$\overline{Y_p} = 0.9771 D^{0.241} \quad \text{for } S = 4\% \tag{26c}$$

$$\overline{Y_p} = 0.9548 D^{0.241} \quad \text{for } S = 6\% \tag{26d}$$

Generally speaking, in the case of a flat upstream bed, the horizontally jet fall down into the downstream due to gravity. However, in the case of a steep upstream bed, in addition to gravity, the steep downward jet accelerates the flow rate in the vertical direction, so as to shorten the impact time/position. Empirical Eqs. (26a)-(26d) confirmed the inferences.

Table 2. Slope effect ratios (SER) for various ICFOF.

Impact characteristics of free over-fall flow with upstream bed slope	Equation of SER δ	Calculated SER for UBS			Relation
		S = 2%	S = 4%	S = 6%	
Dimensionless brink depth $\overline{Y_b}$	$e^{-4.681S}$	0.911	0.829	0.755	negative
Dimensionless impact position $\overline{L_d}$	$e^{6.627S}$	1.142	1.304	1.488	positive
Impact angle θ	$e^{-2.563S}$	0.950	0.903	0.857	negative
Dimensionless tail water depth $\overline{Y_1}$	$e^{-1.780S}$	0.965	0.931	0.899	negative
Dimensionless pool depth $\overline{Y_p}$	$e^{-1.157S}$	0.977	0.955	0.933	negative

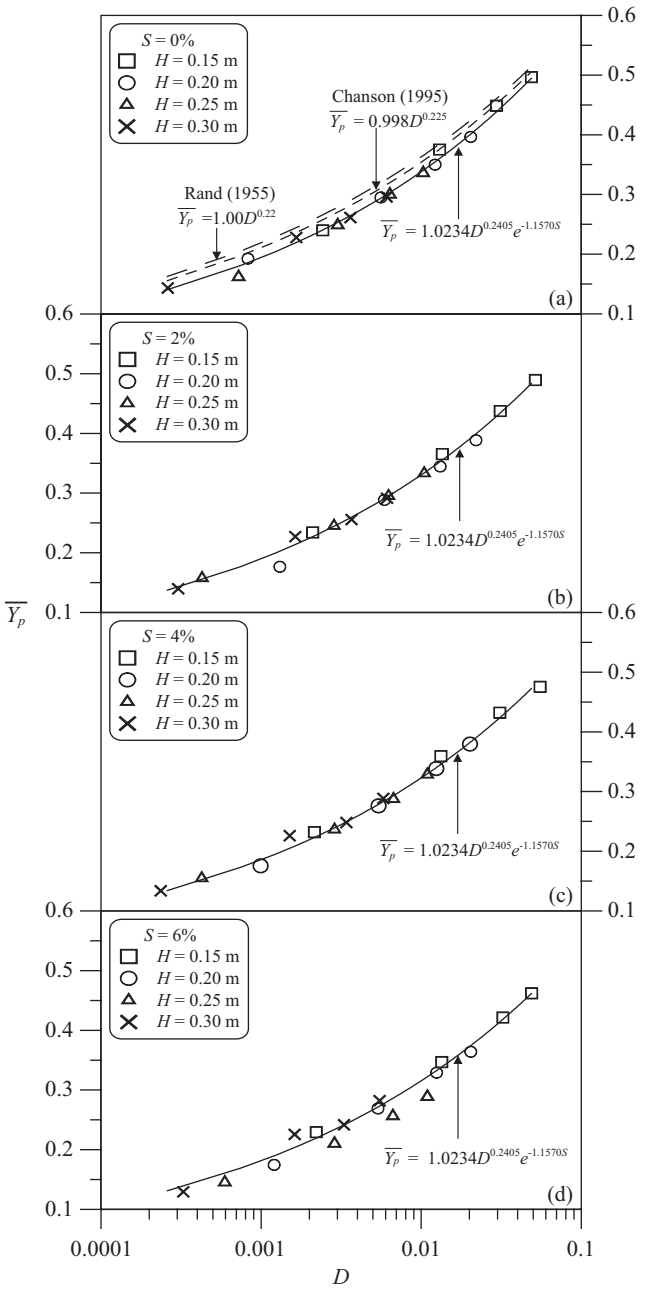

Fig. 8. Variation of dimensionless pool depth with Drop number for various UBS.

6. Depth of Water Pool

Using Eq. (17), the SER for various ICFOF can be obtained. Table 2 gives the Equations. of SER and the corresponding value of SER for various ICFOF with different UBS S. The various impact characteristics of free over-fall vary with UBS S. In Table 2, two types of relationships for ICFOF are defined: one positive and another negative. If the SER for a particular ICFOF increases with an increase in UBS S, such a relationship is defined as a "positive relation". On the other hand, if a particular ICFOF decreases with an increase in UBS S, then it is considered as "negative relation". From Table 2, it can be observed that, except dimensionless impact position all the ICFOF have negative relationship with UBS S.

7. Application of Empirical Equations

Impact position and tailwater depth are useful for the design of downstream apron. The apron length/depth can be determined by the impact position/ tail water depth. Assuming the drop height H = 6.0 m, the width of Sabo dam b = 100 m, the design discharge rate Q = 1,000 CMS, and the UBS S = 0%. The discharge per unit width is

$$q = \frac{Q}{b} = \frac{1{,}000}{100} = 10.00 \ (\mathrm{m^2/s}).$$

The Drop number is

$$D = \frac{q^2}{gH^3} = \frac{10^2}{9.81\times 6^3} = 0.047193 .$$

Using Eq. (20), the impact position is

$$\begin{aligned} L_d &= 1.5303 D^{0.126} \exp(6.627S) H \\ &= 1.5303\times 0.047193^{0.126} \exp(6.627\times 0)\times 6 \\ &= 6.249 \ (\mathrm{m}) \end{aligned}$$

Using Eq. (23), the tail water depth is

$$Y_1 = 0.3779D^{0.362}\exp(-1.780S)H$$
$$= 0.3779\times 0.047193^{0.362}\exp(-1.780\times 0)\times 6$$
$$= 0.751\,(\mathrm{m})$$

V. CONCLUSION

The theoretical equations to predict the impact characteristics of free over-fall (ICFOF) in the pool zone with sloping upstream bed are developed. The impact characteristics considered in the study comprise of the brink depth, the impact position and impact angle, the tail water depth and the depth of water pool. These impact characteristics are expressed in dimensionless forms. The data obtained from the series of laboratory experiments were used to obtain the multiple regression equations for the dimensionless impact characteristics. The results are summarized as follows:

1. The dimensionless brink depth decreases with an increase in upstream Froude number and UBS.
2. The dimensionless impact position, the dimensionless tail water depth and the dimensionless depth of water pool increases with an increase in Drop number.
3. With the increase in UBS, the impact angle, the dimensionless tail water depth and the dimensionless depth of water pool decreases, while the dimensional impact position increases.
4. The empirical relations proposed for previous investigators for horizontal upstream bed were also compared.
5. The slope effect ratio expresses the effect of upstream slope on the various impact characteristics. A large slope effect ratio can induce a large value of impact characteristics of free over-fall flow. The UBS resulting into a large slope effect ratio is considered as "positive relation" to impact characteristics of free over-fall flow, otherwise it is "negative relation". It was found that most of UBS have "negative relation" to impact characteristics of free over-fall flow, except dimensionless impact position.
6. The empirical equations developed in this study can be applied in the practical design of downstream apron such as impact position or tail water depth.

ACKNOWLEDGMENTS

The authors would like to thank the research support from the National Science Council of the Republic of China (project number 102-2313-B-451-001 and 99-2221-E-005-044).

NOTATION

The following symbols are used in this paper:

a, b, c = constants [–];
D = Drop number, q^2/gH^3 [–];
d_a = width of outside part of nappe [L];
d_b = width of inside part nappe [L];
d_f = depth of water jet deflected into the water pool [L];
F_0 = upstream Froude number $u_0/\sqrt{gY_0\cos\varphi}$ [–];
g = gravitational acceleration [LT^{-2}];
H = drop height [L];
L_d = impact position [L];
$\overline{L_d}$ = dimensionless impact position, L_d/H [–];
q = discharge per unit width [L^2T];
q_f = discharge per unit width from water pool [L^2T];
S = upstream channel slope, tan φ [–];
t = time [T];
u = impacting velocity of water nappe on downstream of drop [LT^{-1}];
u_b = velocity at drop edge [LT^{-1}];
u_c = critical velocity [LT^{-1}];
u_m = average velocity in mixing section of nappe and repeated rotary flow of water pool [LT^{-1}];
X = horizontal coordinate of impact position of nappe from drop edge [L];
Y = vertical coordinate of impact position of nappe from drop edge [L];
Y_0 = upstream water depth [L];
Y_1 = tail water depth [L];
$\overline{Y_1}$ = dimensionless tail water depth, Y_1/H [–];
Y_b = brink depth [L];
$\overline{Y_b}$ = dimensionless brink depth, Y_b/Y_c [–];
Y_c = critical water depth [L];
Y_p = pool water depth [L];
$\overline{Y_p}$ = dimensionless depth of water pool, Y_p/H [–];
y = nappe depth impacting on downstream side of drop [L];
Z_n = water surface elevation above drop edge at measured position of upstream water depth [L];
α = energy correction coefficient [–];
β = momentum correction factor [–];
δ = slope effect ratio $A_{(S>0)}/A_{(S=0)}$ [–];
φ = inclination of upstream bed [–];
θ = impact angle [–]; and
ρ = water density [ML^{-3}];

REFERENCES

1. Chamani, M. R. and Beirami, M. K., "Flow characteristics at drops," *Journal of Hydraulic Engineering*, Vol. 128, No. 8, pp. 788-791 (2002).
2. Chanson, H., *Hydraulic Design of Stepped Cascades, Channels, Weirs and Spillways*, Pergamon Press, New York (1995).
3. Chen, J. Y. and Hong, Y. M., "Characteristics of check dam scour hole by free over-fall flow," *Journal of Chinese Institute Engineering*, Vol. 24, No. 6, pp. 673-680 (2001).
4. Chen, J. Y., Huang, H. S., Hong, Y. M., and Liu, S. I., "The impact characteristics analysis of free over-fall flow on downstream channel bed," *Journal of Chinese Institute Engineering*, Vol. 34, No. 3, pp. 403-413 (2011).

5. Chen, S. W., *Experimental Study of Riverbed Girdle Arrangements in the Downstream of Sabo Dam*, Master Thesis, Department of Civil Engineering, National Chung Hsing University, Taichung, Taiwan (2002).
6. Davis, A. C., Ellett, B. G. S., and Jacob, R. P., "Flow measurement in sloping channels with rectangular free overfall," *Journal of Hydraulic Engineering*, Vol. 124, No. 7, pp. 760-763 (1998).
7. Hong, Y. M., Huang, H. S., and Wan, S., "Drop characteristics of free-falling nappe for aerated straight-drop spillway," *Journal of Hydraulic Research*, Vol. 48, No. 1, pp. 125-129 (2010).
8. Ippen, P. J., *Engineering Hydraulic*, John Wiley and Sons, Inc., New York (1943).
9. Rand, W., "Flow geometry at straight drop spillways," *Journal of Hydraulic Engineering*, Vol. 81, pp. 1-13 (1955).
10. Shiu, Y. H., *A Study of Hydraulic Characteristics of Supercritical Free Overfall Impact*, Master Thesis, Department of Civil Engineering, National Chung Hsing University, Taichung, Taiwan (2010).
11. Stein, O. R. and Julien, P. Y., "Sediment concentration below free overfall," *Journal of Hydraulic Engineering*, Vol. 120, pp. 1043-1059 (1994).
12. Tokyay, N. D. and Yildiz, D., "Characteristics of free overfall for supercritical flows," *Canada Journal of Hydraulic Engineering*, Vol. 34, No. 2, pp. 162-169 (2007).
13. White, M. P., "Discussion on energy loss at the base of a free over-fall," *Transactions American Society of Civil Engineering*, Vol. 108, pp. 1361-1364 (1943).